

# Numerical Simulation of the Passenger Side Airbag Deployment in Out-of-Position

Driss Bendjaballah, Ali Bouchoucha and Mohamed Lakhdar Sahli

**Abstract** In recent years many accidents happened with passengers that were out of position when their airbag deployed. Therefore new safety regulations have come into effect and an airbag now has to meet several requirements that concern out of positioning. In meeting these requirements simulations of folding and deploying airbags are very useful and are widely used. The paper presents a simulation method for the deploying airbags using three materials in different working conditions. The deploying modeling of passenger side airbag is a complex and time consuming process. In these simulations the gas flow is described by the conservation laws of mass, momentum and energy. The main aim of this study is evaluate the performance of deploying of passenger side airbag using Finite Element Methods (FEM).

**Keywords** Airbags · Crash · Finite element simulations · Modeling · Out-of-position

## 1 Introduction

Nowadays, occupant safety is one of the principal objectives in the design of vehicles. Numerous innovations have appeared in recent years aimed at increasing safety in vehicles [1–3]. As is well known, airbags, like safety belts are now devices

---

D. Bendjaballah (✉) · A. Bouchoucha · M.L. Sahli  
Mechanics Laboratory, Faculty of Technology Sciences,  
Mentouri Brother University, Constantine, Algeria  
e-mail: d\_bendjaballah@hotmail.fr

A. Bouchoucha  
e-mail: bouchoucha\_ali1@yahoo.fr

M.L. Sahli  
e-mail: Mohamed.sahli@femto-st.fr

M.L. Sahli  
Femto-St Institute, Applied Mechanics Department,  
CNRS UMR 6174, Besançon, France

designed to provide protection to the users of vehicles during crash events, minimizing the loads necessary to adapt their movement to the movement of the car [4, 5]. In general, the seat belt is designed to restrain the occupant in the vehicle and prevent the occupant from having harsh contacts with interior surfaces of the vehicles. The airbag acts to cushion any impact with vehicle structure and has positive internal pressure, which can exert distributed restraining forces over the head and face. Furthermore, the airbag can act on a wider body area including the chest and head, thus minimising the body articulations, which cause injury [6]. These safety elements can so reduce the death rates on the roads, and its protection effects have been widely approved [7, 8]. Thus, new types of airbag products are being developed to handle different collision scenarios.

In recent years, occupant protection airbags have become standard equipment on most new passenger vehicles [9–11]. The airbag cushion is composed of a woven fabric which is rapidly inflated during a car crash. The airbag dissipates the passenger's kinetic energy thereby reducing injury through biaxial stretching of the fabric bag and escaping gas through vents. Therefore, the performance of the airbag is greatly influenced by the mechanical properties of the fabric. Generally, air bags are designed to deploy in a crash that is equivalent to a vehicle crashing into a solid wall at 8 to 14 miles per hour. Air bags most often deploy when a vehicle collides with another vehicle or with a solid object like a tree. There are various types of airbags; frontal, side-impact and curtain airbags. In general, the passenger side airbags are usually larger than the driver airbags (see Fig. 1).

Extensive studies have shown that the airbag deployment in load cases consists of two occupant loading phases: a punch-out effect where the airbag bursts out of its container with the airbag and airbag module cover accelerating towards the occupant, and a second loading phase during which the airbag is taking on its deployed shape and volume (membrane-loading effect). Bankdak et al. (2002) developed an experimental airbag test system to study airbag-occupant interactions during close proximity deployment. The results provided insight for simulating the effect of inflation energy and mass flow on target response [13]. Bedard et al. (2002) found that while left-side (driver-side) impacts accounted for only 13.5 % of all crashes, the fatality rate among these crashes was 68.3 % in comparison to front impact (48.3 %), right-side impact (31.3 %), and rear impact (38.4 %). These studies underscore the importance of occupant safety during side impact collisions [14]. In the last years, current market request to reduce the time and cost airbag development. In order to achieve this result, virtual simulations play an important role since

**Fig. 1** Frontal and side airbags [12]



they allow to minimize the number of experimental tests [15, 16]. Several simulation models of airbag were established [17]. It's feasible to optimize the parameters of airbag deployment using simulation technology. Experimental and numerical studies have quantified injury risks to close-proximity occupants from deploying side airbags. These studies have focused on the prevention of the most adverse effects of airbag deployment [18]. Other studies have proposed airbag characteristics to minimize particular biomechanical responses [19]. In a more recent study, Marklund and Nilsson (2003) compared deformation patterns with experimental data as well as the computational costs associated with three different airbag deployment simulation methods; they concluded that the SPH method is relatively inexpensive and produces incremental deformation patterns that compare most closely to the experimental results [20]. The process of inflation of an airbag is one of the determining factors in saving lives. The duration from the initial impact of the crash to the full inflation of an airbag is about 40 ms and during this time, the airbag goes from being in a folded state to a fully inflated state, with a high internal pressure. After achieving this state, the airbag begins to deflate, thus providing a nice cushion for the body impacting it. Ideally the person in the crash should come into contact with the airbag at this time. This study is therefore mainly focused on the numerical simulation of the passenger airbag, without taking into account the effects of a folding of airbag and the crash dummy, let's understand the one first. The main aim of this study is evaluate the performance of deploying of passenger side airbag using Finite Element Methods (FEM).

## 2 Finite Element Model of Airbag Simulation

### 2.1 Theoretical Background

Numerical simulations of airbags use very complex and techniques such as, an orthotropic model to identify the mechanical behaviors during the airbag inflation, the fluid mechanics (gas flow) to describe the inflator gas flow (pressure gradient), and improve the representation of the pressures within the airbag. To model the airbag as an orthotropic model, three material constants have to be provided. Assuming a plane stress condition, the material constitutive equations are given by [21]:

$$\begin{Bmatrix} \sigma_1 \\ \sigma_2 \\ \tau_{12} \end{Bmatrix} = \begin{pmatrix} Q_{11} & Q_{21} & 0 \\ Q_{12} & Q_{22} & 0 \\ 0 & 0 & Q_{66} \end{pmatrix} \cdot \begin{Bmatrix} \varepsilon_1 \\ \varepsilon_2 \\ \gamma_{12} \end{Bmatrix} \quad (1)$$

where  $\sigma$  is the normal stress and  $\tau$  is the shear stress, the subscript refers to the principal material directions, i.e. the fill and warp directions. Also  $\varepsilon$  and  $\gamma$  are the strain components. The material elastic constants  $Q_{ij}$  are given by the following equations:

$$\begin{aligned} Q_{11} &= \frac{E_1}{1-\nu_{12} \cdot \nu_{21}}, & Q_{12} &= \frac{\nu_{12} \cdot E_2}{1-\nu_{12} \cdot \nu_{21}} = \frac{\nu_{21} \cdot E_2}{1-\nu_{12} \cdot \nu_{21}} \\ Q_{22} &= \frac{E_2}{1-\nu_{12} \cdot \nu_{21}}, & Q_{66} &= G_{12} \end{aligned} \quad (2)$$

where  $E_1$  and  $E_2$  are the Young's modulus in the fill and wrap directions and  $G_{12}$  is the shear modulus of the fabric material.  $\nu_{ij}$  is the Poisson ratio of the material.

The gas exerts a pressure load on the airbag causing it to expand. This expansion puts the airbag under tensile stress lowering the expansion rate. In this study, heat conduction and heat transfer is not taken into account. In the deployment of an airbag an inflator supplies high velocity gas into an airbag causing it to expand rapidly. The gas inside the airbag is assumed to be ideal, to be of constant entropy and to satisfy the equation of state:

$$p = (\gamma - 1) \cdot \rho \cdot e \quad (3)$$

Here  $p$ ,  $\rho$  and  $e$  are respectively the pressure, density, specific internal energy and  $\gamma$  is the ratio of the heat capacities of the gas. The gas flow is described by the conservation laws for mass, momentum and energy that read:

$$\begin{aligned} \frac{d}{dt} \int_V \rho dV + \int_A \rho(u \cdot n) dA &= 0 \Rightarrow \frac{d}{dt} \int_V \rho u_i dV + \int_A \rho u_i (u \cdot n) dA \\ &= - \int_A p n_i dA \\ \Rightarrow \frac{d}{dt} \int_V \rho e dV + \int_A \rho e (u \cdot n) dA &= - \int_A u_i p n_i dA \end{aligned}$$

Here  $V$  is a volume;  $A$  is the boundary of this volume,  $n$  is the normal vector along the surface  $A$  and  $u$  denotes the velocity vector in the volume. Applying Bernoulli's equation in the case of an ideal gas with constant entropy gives:

$$\frac{1}{2} u^2 + \frac{\gamma}{\gamma - 1} \frac{p}{\rho} = \frac{1}{2} u_{ex}^2 + \frac{\gamma}{\gamma - 1} \frac{p_{ex}}{\rho_{ex}} \quad (5)$$

Here the subscript  $ex$  denotes quantities at the throat of the tube. Furthermore  $u$ ,  $p$  and  $\rho$  denote the quantities inside that part of the tube that is supplying mass. This gives

$$u_{ex}^2 = \frac{2\gamma}{\gamma - 1} \left( \frac{p}{\rho} - \frac{p_{ex}}{\rho_{ex}} \right) \quad (6)$$

## 2.2 Materials and Boundary Conditions

The airbag system mainly consists of three parts: the airbag itself, the inflator unit and the crash sensor or diagnostic unit. Thus, to study the behavior of the airbag using FE simulations, we need to have an FE model of the airbag in the folded position. A FE model of the airbag was used to simulate the test condition as shown in Fig. 2. LS-DYNA<sup>®</sup> material model FABRIC (MAT\_34) is used to simulate the airbag material. It is a variation of the layered orthotropic material model [22]. Additionally in the LS-DYNA<sup>®</sup> material model, fabric leakage can be accounted for. However, for this CAB material, the leakage is almost negligible and therefore no leakage is specified. The mechanical properties can be determined from the physical test. Typical material properties for airbag fabrics are taken as given in Chawla et al. (2004). These properties are used to simulate inflation process of airbag (see Table 1). The car dashboard is modeled as the rectangular thin plate using a MAT\_RIGID material and the degrees of freedom are constrained in all the directions. It is assigned the similar properties of thermoplastic polymer for contact purposes. The porosity of the fabric is assumed zero. The Nitrogen gas is taken for inflating the airbag. Properties of nitrogen gas and initial bag conditions are shown in Table 2. The example on which we perform the study is a typical passenger side airbag. The geometric details have been measured from a commercially available airbag. The initial state of the airbag is a closed rectangular whose sides are to be finished to 482\*635 mm<sup>2</sup>, and is shown in Fig. 2.

Airbag mesh is generated in Ansys<sup>®</sup> Finite Element Software. It consists of 2832 elements and 2875 nodes in the airbag mesh. Quadrilateral elements are used for airbag mesh. The airbag mesh is exported to Lsdyna<sup>®</sup> software (see Fig. 3). All the simulations of the airbag deployment mesh are done in this software. Contact

Fig. 2 The initial airbag geometry in the form of a rectangular

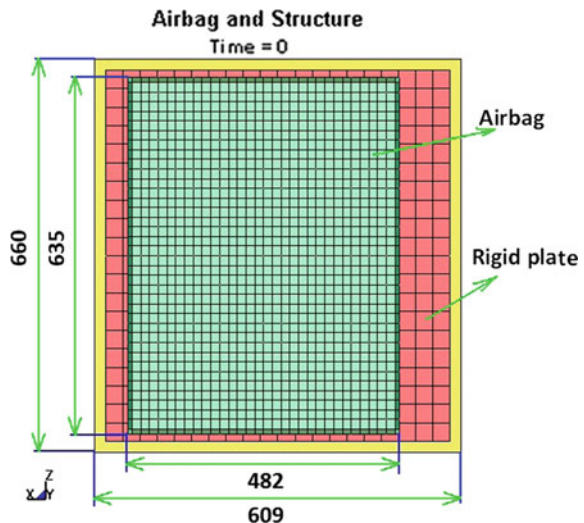


**Table 1** Material properties of airbag and rigid plate considered in the FE simulations [23]

Materials	Airbag	Rigid plate
Density of fabric ( $\text{g/cm}^3$ )	1.02	7.84
Young's modulus (GPa)	13.8	206
Poisson's ratio	0.35	0.30
Shear modulus (GPa)	6.9	–

**Table 2** Initial values used for FE simulation of the swelling of passenger airbag [24]

Pressure (Pa)	$10^4$
Temperature ( $^{\circ}\text{C}$ )	25
Universal gas constant ( $\text{kg/kmol K}$ )	8.314
Initial pressure (Pa)	$1.01 \times 10^4$
Molecular weight ( $\text{kg/mol}$ )	0.02802
Added initial volume ( $\text{m}^3$ )	$3.33 \times 10^{-4}$

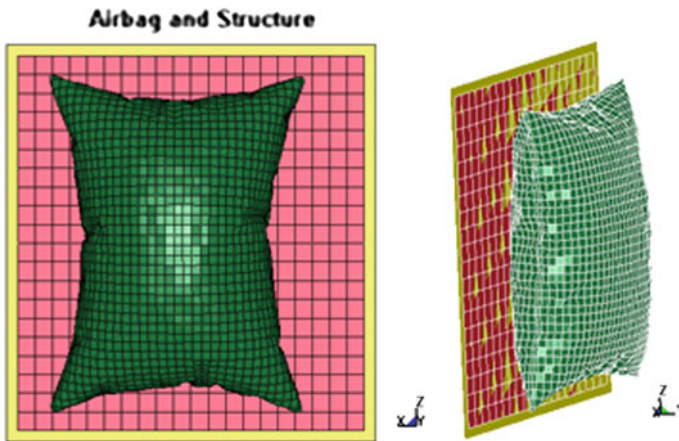


**Fig. 3** Top view and isometric view of inflated airbag and rigid plate meshes

type 37 of Lsdyna<sup>®</sup> software is used for defining the contact between airbag mesh and rigid plates. This contact type is between node and surface. Airbag mesh is treated as nodes and rigid plates are taken as surface. In the simulation, the pressure generated by the gas is then uniformly applied to the internal surface of the airbag fabric.

In the simulation there will be an airbag surface and gas that fills up the inside of this surface. The airbag surface consists of flexible membrane elements that deform under tensile stresses and cannot carry compressive loads. The airbag control volume in LS-DYNA<sup>®</sup> is modeled as an AIRBAG\_SIMPLE\_AIRBAG\_MODEL to simulate the air test condition. A baseline model of the airbag is run using AIRBAG\_LOAD\_CURVE option. This gives an estimate of the volume of the airbag.

### 3 Numerical Results and Discussions

Figure 4 shows the different steps of the deploying airbags test simulation at different time points. Due to the fact that only 11 ms are simulated, the airbag is fully inflated as can be seen in Fig. 4. From the Figures, it can be seen that the airbag module cover opens fully, as close to reality. The increasing of volume is coming mainly from the gas flow.

Figure 5 shows the displacements result during the airbag deployment versus time values. Initially, the both surfaces of the airbag are close and parallel, then as the maximum displacement estimated is the same one with low values recorded near the corners of the structure. Then there are concentrated little by little towards the center of the airbag. The final results of the swelling contours are characterized by a symmetric displacement. The final y-y effective strain contours computed are plotted in Fig. 6. As shown this figure, a state of deployment and swelling of passenger airbag with highly non-uniform deformation is detected around the bag. In the present analysis, the localized elastic strains reach values far below the rupture strain that can be measured in the tensile test [25]. Nevertheless, according to the global material response, the constitutive model is found to be still valid at such high deformation levels. Moreover, the development of plaiice can clearly be seen during the swelling of passenger airbag.

The airbag result displaces and average pressure distribution inside the airbag for four different thicknesses, 100, 150, 200 and 250  $\mu\text{m}$  is depicted in Fig. 7. They represent the end of swelling of passenger airbag, the final geometry of the bag and the contour of pressure of the gas inside the bag. We can observe how not only the development of plaiice of airbag, but also the distribution of pressure is quite different from one case to another. In particular, we can see how the configuration 4

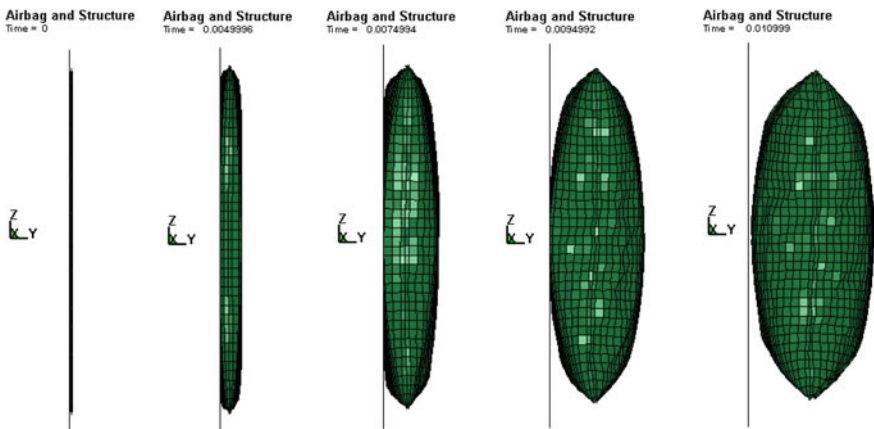


Fig. 4 Airbag deployment at  $t = 11$  ms



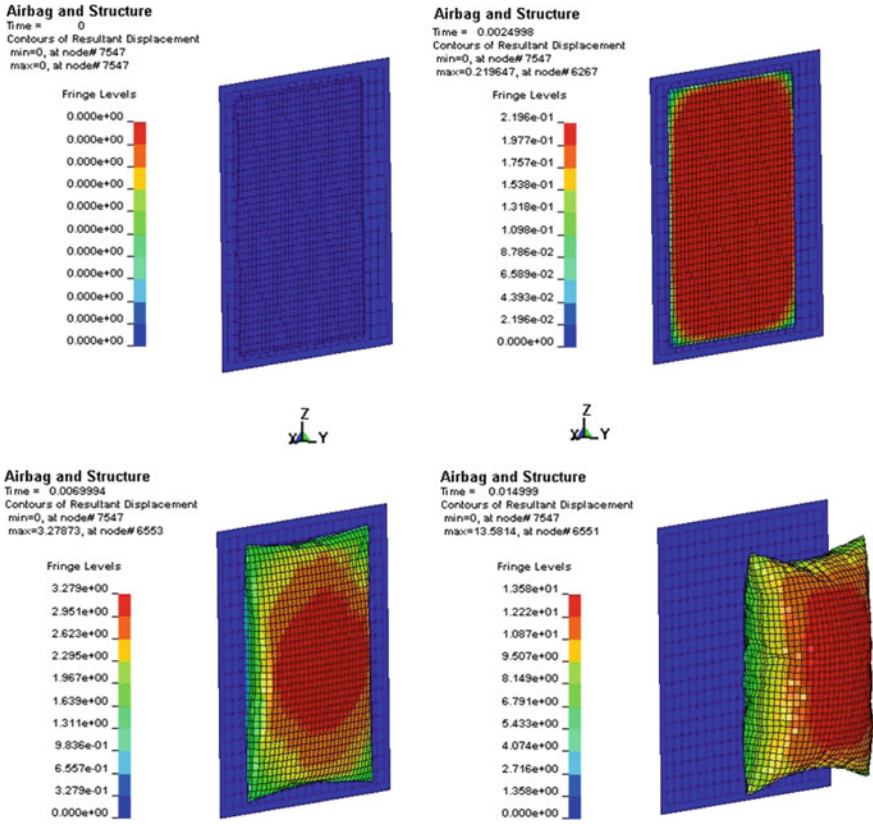


Fig. 5 Airbag result displace

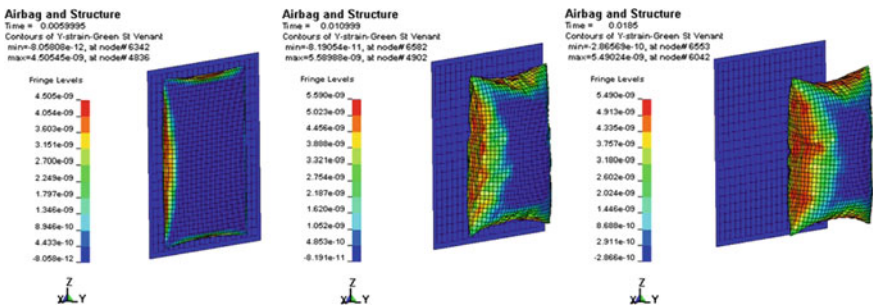


Fig. 6 Airbag result of strain y-y



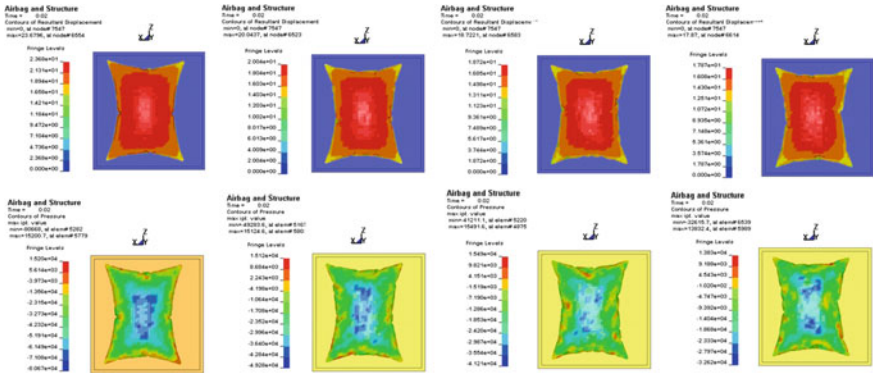


Fig. 7 Airbag result displaces and pressure using different thickness

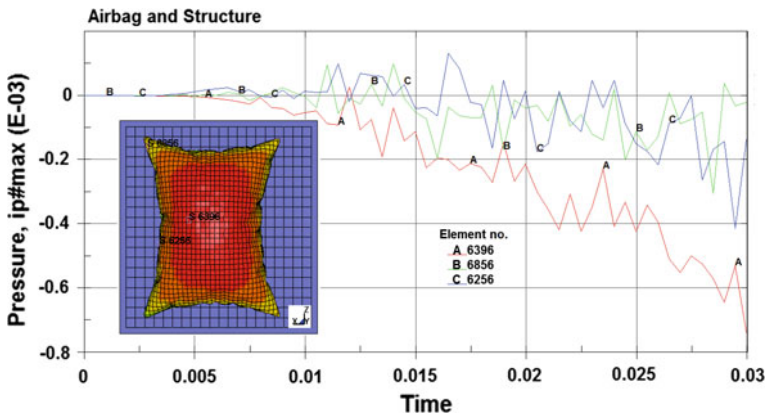


Fig. 8 Pressure evolution versus time

deploys much less aggressively than, for instance, the configuration 1. In this case, there is a quick evolution of the volume and the pressure at the same time [26].

The resulting pressure curves versus time of swelling airbag are plotted in Fig. 8 where the computed responses of different critical zones are apparent. As expected, during the swelling airbag phase, the maximum pressure values are saved at middle of the structure. Moreover, we have also seen after 30 ms, the ratio between the maximum pressure differences is around 28 %. This difference is significantly dependent of the geometric form of airbag [26]. Figure 9 shows the energy total of the system vs. time history during the deploying of the airbag. Maximum value observed at time 30 ms. They increase significantly with the gas injection pressure in bag. The total energy during the swelling airbag can be used to absorbed the collision during crash, by the cushioning effect provided by the airbag, and by the deflation of the inflated airbag, which occurs due to the holes provided in the airbag fabric.

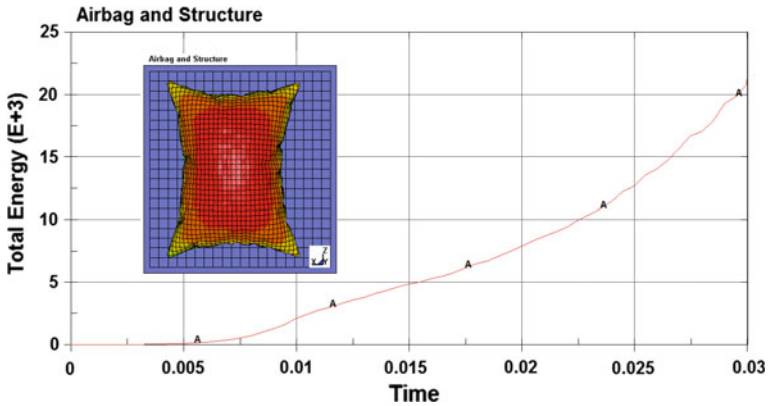


Fig. 9 Total energy versus time during the swelling airbag

## 4 Conclusions

The study investigated into the effect of airbag deployment in normal scenario without taking into account in this work of the presence of the occupants of various masses and statures. The results first has allowed us to shown that airbag has been modelled correctly with a proper filling of the gas flow. The numerical results shown that the method presented in this paper is also a promising method for simulating airbags but nevertheless some improvements were needed in the modelling of the cover (including the cover thicknesses and mesh boundary conditions) and the tear seam (including the tear seam geometry and the failure method). Besides that, physical tests will also conducted and simulated to assess the different scenarios. Further testing with real life airbags and comparison with experiments is required. It is also very important to model proper folding for airbag mesh for studying contact interaction of out-of-position users with an inflating airbag. These will be carried out in the near future.

## References

1. Zhang, H., et al.: CAE-based side curtain airbag design. In: SAE 2004-01-0841, SAE World Congress, 8–11 March 2004, Detroit, Michigan, 8–11 March (2004)
2. Soongu, H.: A study on the modeling technique of airbag cushion fabric. In: SAE 2003-01-0512, SAE World Congress, 3–6 March 2003, Detroit, Michigan, 3–6 March (2003)
3. Canaple, B., et al.: Impact model development for the reconstruction of current motorcycle accidents. *Int. J. Crash* **7**, 307–320 (2002)
4. Freesmeyer, J.J., Butler, P.B.: Analysis of a hybrid dual-combustion-chamber solid propellant gas generator. *J. Propuls. Power* **15**, 552–561 (1999)

5. Schmitt, R.G., Butler, P., Freesmeyer, J.: Performance and CO production of a non-azide airbag propellant in a pre-pressurized gas generator. *Combust. Sci. Technol.* **122**, 305–350 (1997)
6. Gabauer, D.J., Gabler, H.C.: The effects of airbags and seatbelts on occupant injury in longitudinal barrier crashes. *J. Saf. Res.* **41**, 9–15 (2010)
7. Crandall, C.S., Olson, L., Sklar, D.P.: Mortality reduction with air bag and seat belt use in head-on passenger car collisions. *Am. J. Epidemiol.* **153**, 219–224 (2001)
8. Teru, I., Ishikawa, T.: The effect of occupant protection by controlling airbag and seatbelt. In: *Proceedings of the 18th International Technical Conference on the Enhanced Safety of Vehicles*. NHTSA, Nagoya, Japan (2003)
9. Braver, E.R., Kyrychenko, S.Y.: Efficacy of side airbags in reducing driver deaths in driver-side collisions. *Am. J. Epidemiol.* **159**, 556–564 (2004)
10. Teng, T.L., Chang, K.C., Wu, C.H.: Development and validation of side-impact crash and sled testing finite-element models. *Veh. Syst. Dyn.* **45**, 925–937 (2007)
11. Yoganandan, N., Pintar, F., Zhang, J., Gennarelli, T.A.: Lateral impact injuries with side airbag deployments—a descriptive study. *Accid. Anal. Prev.* **39**, 22–27 (2007)
12. Lim, J.-H., Park, J., Yun, Y.-W., Jeong, S., Park, G.: Design of an airbag system of a mid-sized automobile for pedestrian protection. *J. Automob. Eng.* 21–33 (2014)
13. Bankdak, F.A., Chan, P.C., Lu, Z.: An experimental airbag test system for the study of airbag deployment loads. *Int. J. Crashworthiness* **7**, 129–161 (2002)
14. Bedard, M., Guyatt, G.H., Stones, M.J., Hirdes, J.P.: The independent contribution of driver, crash and vehicle characteristics to driver fatalities. *Accid. Anal. Prev.* **34**, 717–727 (2002)
15. Pei, J., Yuan, S.Q., Yuan, J.P.: Numerical analysis of periodic flow unsteadiness in a single-blade centrifugal pump. *Sci. China Technol. Sci.* **56**, 212–221 (2013)
16. Cao, Y.H., Wu, Z.L., Huang, J.S.: Numerical simulation of aerodynamic interactions among helicopter rotor, fuselage, engine and body of revolution. *Sci. China Technol. Sci.* **57**, 1206–1218 (2014)
17. Wang, Y.E., Yang, C.X., Peng, K.: Airbag cushion process simulation for cargo airdrop system. *J. Syst. Simul.* **19**, 3176–3179 (2007)
18. Duma, S.M., Boggess, B.M., Crandall, J.R., Hurwitz, S.R., Seki, K., Aoki, T.: Upper extremity interaction with a deploying side airbag: a characterization of elbow joint loading. *Accid. Anal. Prev.* **35**, 417–425 (2003)
19. Haland, Y., Pipkorn, B.: A parametric study of a side airbag system to meet deflection based criteria. *J. Biomech. Eng.* **118**, 412–419 (1996)
20. Marklund, P.O., Nilsson, L.: Optimization of airbag inflation parameters for the minimization of out of position occupant injury. *Comput. Mech.* **31**, 496–504 (2003)
21. Jones R.M.: *Mechanics of Composite Materials*. Hemisphere Publishing Corporation (1975)
22. LS-DYNA3D User's Manual version 970
23. Chawla, A., Bhosale, P.V., Mukherjee, S.: Modeling of folding of passenger side airbag mesh. *SAE Int.* 1–8 (2004)
24. Deery, H., Morris, A.P., Fildes, B., Newstead, S.: Airbag technology in Australian passenger cars: preliminary results from real world crash investigations. *J. Crash Prev. Inj. Control* **1**, 121–128 (1999)
25. Wu, W.T., Hsieh, W., Huang, C.H., Wang, C.H.: Theoretical simulation of combustion and inflation processed of two-stage airbag inflators. *Combust. Sci. Technol.* **117**, 383–412 (2005)
26. Blundell, M., Mahangare, M.: Investigation of an advanced driver airbag out-of-position injury prediction with Madymo gas flow simulations. In: *Madymo User Meeting* (2006)